# Graph based Method for Enhanced Heart Rate Trace Estimation using UWB Impulse Radar

Hui Tang, Xueqin Liu
*School of Information Science and Engineering*
*Wuhan University of Science and Technology*
Wuhan, China
htang@wust.edu.cn

Yu Rong and Daniel Bliss
*School of Electrical, Computer and Energy Engineering*
*Arizona State University*
Tempe, AZ, USA
yrong5@asu.edu

***Abstract*—In this paper, we propose a graph based method to improve the heart rate trace estimation in UWB impulse radar. The key idea is to extract the heart rate from spectrograms using graph weight and normalised cuts image segmentation. Radar heartbeat signal is generally weak and inevitably couple with motion interference including involuntary body motion and respiration. When the pulse signal to interference plus noise ratio is low, the graph-based method outperforms the conventional spectral peak finding method. The spectrograms by complex data has better estimation performance than phase data. The harmonic signal promoted by complex data is helpful to the heart rate estimation when the fundamental heart rate signal is weak or masked by respiration interference. We validate the graph-based method through experimental demonstration.**

***Index Terms*—heart rate estimation, graph, segmentation, UWB radar**

## I. Introduction

Detecting human vital sign using short-range radar technology is an important application in health development [1], [2]. The non-invasive detection of vital sign has led to several potential applications such as elderly-care and in-hospital monitoring. Heart rate is one of the most important vital sign parameters that can be used to inspect potential health issues. By continuous monitoring the heart rate, we can check the changes of our resting heart-rate.

Ultra-wide band (UWB) radar system has strong penetrating ability compared to optical systems, and fine range resolving ability compared to continuous wave (CW) radar systems [3], [4]. UWB radar using an impulse or frequency modulated signal can non-invasively monitor internal physiological motion of the organs of a body such as heartbeat, lung, blood flooding. In [5], they have discussed the effectiveness of monitoring vital sign of stationary human subject in a remote manner using UWB radar.

Various signal processing techniques have been developed for Doppler-based vital signs detection. The popular complex signal demodulation (CSD) method [6] fails when the lower order-harmonics of respiration is close to the fundamental heartbeat in the spectral domain. Phase-based method [7] and its variants [8] fail when the phase noise cannot be correctly compensated. In real system, an automatic phase calibration procedure is still unknown. Harmonic signatures are utilized to recover the fundamental heartbeat frequency from its higher-order spectral features [9], [10], which do not need the phase information. They point out that spectrally the fundamental heartbeat frequency is respiration-interference limited. The main challenge of monitoring fundamental heartbeat continuously is due to the spurious spectrum peaks such as 2nd or 3rd-order harmonics of respiration. Due to weak heartbeat amplitude and measurement noise, the accurate measurement of the target heart rate is still a challenge.

Segmentation is the separation of images into more meaningful information based on similarity or difference, continuity or discontinuity. Segmentation using graph cut methods, depends on assignment of appropriate weights. The paths are obtained by the default shortest path algorithms. Graph-cut is an optimization method used in solving many image processing and computer vision problems, where the problem is represented as a graph. [11] was originally developed for segmenting the retinal layers in the cross-sectional images from Optical Coherence Tomography.

It is inspiring to handle the heart rate estimation problem from the view of image segmentation. The spectrogram images by the time-frequency analysis Short-time Fourier transform (STFT) contains obvious layered structures of vital sign signal. Vital sign estimation is to capture frequency components of a signal vary over time in their spectrograms. In [12], they reported an image segmentation-based heart rate extraction method in FMCW radar, which expanded the scope of retinal layer segmentation algorithms to the field of spectral analysis. Motivated by this, this paper extends this graph based method to enhance heart rate trace estimation using UWB pulse radar.

**Our contribution**:

- according to the authors' knowledge, we are the first to utilize the graph-based method to estimate the heart rate in UWB impluse radar
- we experimentally demonstrate the effectiveness of the graph-based method

## II. Signal Model

In this section, we discuss the signal model for vital sign detection using UWB impulse radar. We summarize the results

This paper was supported by the National Natural Science Foundation of China under grant 62173259, the Natural Science Foundation of Hubei Province (No. 2022CFB110)

in reference [9]. The received signal is directly sampled in RF and then digitally converted to the complex baseband. In our model, $\tau$ denotes the fast sampling time and $v$ is the transformed frequency component, while $t$ denotes the slow cross-range sampling time and $f$ denotes the corresponding Fourier domain component. The vital signs of a subject at a nominal distance $d_0$ can be modeled as a sum of two periodic signals from respiratory and cardiac activities,

$$d(t) = d_0 + M_b sin(2\pi f_b t) + M_h sin(2\pi f_h t), \tag{1}$$

where $M_b$ is the amplitude of respiratory activity, and $M_h$ is the amplitude of cardiac activity. $f_b$ and $f_h$ are respiration and heartbeat frequencies.

The received signal can be modeled as a sum of the target response and the delayed, attenuated versions of the transmitted pulse due to static environment,

$$r(t,\tau) = A_T p(\tau - \tau_D(t)) + \sum_i A_i p(\tau - \tau_i), \tag{2}$$

where $p(t,\tau)$ is the generated short pulse, centered at the carrier frequency $F_c$. $A_T$ and $A_i$ denote the magnitude of the target response and the multi-path components, while $\tau_D(t) = 2d(t)/c$ and $\tau_i$ are the corresponding delays, where $c$ is the speed of light.

The signal of interest can be modeled as,

$$r_0(t,\tau) = A_T p(\tau - \tau_D(t)), \tag{3}$$

where the multi-path components due to static environment can be eliminated by mean subtraction.

The received signal is then down converted to the complex baseband and represented as,

$$\begin{aligned} y(t,\tau) &= r_0(t,\tau) e^{-j2\pi F_c \tau} \\ &= A_T p(\tau - \tau_D(t)) e^{-j2\pi F_c \tau}. \end{aligned} \tag{4}$$

We also show how to extract phase variation due to vital sign activity. For convenience, we evaluate the fast-time Fourier transform applied to Eqn.(4) at DC is

$$Y(t,0) = A_T M_P e^{-j(2\pi F_c \tau_D(t) + \phi_P)}. \tag{5}$$

where $M_P$ and $\phi_P$ are the magnitude and phase of the fast-time Fourier transform of the transmitted pulse shifted to DC.

Note that $A_T$ and $M_P$ are real numbers and the vital information is preserved in the phase term. The I and Q channels can be represented as,

$$I(t) = A_T M_P cos(2\pi F_c \tau_D(t) + \phi_P), \tag{6}$$

$$Q(t) = A_T M_P sin(2\pi F_c \tau_D(t) + \phi_P), \tag{7}$$

By directly calculate the phase shift as a Arctangent function of $Q(t)/I(t)$, the accurate phase variation extraction is possible,

$$\Phi(t) = \text{unwrapping}\{\text{atan}(\frac{Q(t)}{I(t)})\}. \tag{8}$$

## III. Methodology

In this section, we describe the proposed heart rate trace estimation method. The signal processing flow chat is shown in Fig. 1. The algorithm is generalised for layered structure segmentation, which is an ideal method for extracting the vital signs in STFT spectrograms. An open source retinal layer segmentation software is adopted for the spectral analysis application [13].

The vital spectrogram is computed using STFT [14], [15]. Let $x(t)$ denote the signal to be analyzed, its STFT is written as,

$$X(\tau,\omega) = \int_{-\infty}^{\infty} x(t) w(t-\tau) e^{-i\omega t} dt \tag{9}$$

where $\omega(\tau)$ is the window function. The magnitude squared of the STFT yields the spectrogram $S(\tau,\omega)$,

$$S(\tau,\omega) \equiv |X(\tau,\omega)|^2 \tag{10}$$

where $X(\tau,\omega)$ is the Fourier transform of $x(t)\omega(t-\tau)$, a complex function representing the phase and magnitude of the signal over time and frequency.

Each spectrogram is treated as an image. Given an image $I$ with $n \times n$ pixels, we convert it into an undirected and connected graph $\mathcal{G} = (\mathcal{V}, \mathcal{E}, \mathbf{W})$. $\mathcal{V}$ is a finite set of $|\mathcal{V}| = n^2$ vertices, where each node is corresponding to a pixel. $\mathcal{E}$ is a finite set of edges, denoted as $e = (v_s, v_t) \in \mathcal{E}$, which are decided by their neighbors. The adjacency matrix $\mathbf{W} \in \mathbb{R}^{n^2 \times n^2}$ represents the mapping association between nodes.

When cutting a graph into segments, a route between the start and the end nodes needs to be created by assigning weights to edges. In the spectrograms, the signals to be extracted are layer-like and primarily horizontal [12]. Therefore, the difference in intensity can be represented by finding the vertical gradients of the image:

$$w_{st} = 2 - (g_s + g_t) + w_{min} \tag{11}$$

Where $g_s$ and $g_t$are the vertical gradients of the image at node $s$ and $t$, respectively. $w_{st}$ is the weight assigned to node $s$ and $t$, and $w_{min}$ is the minimum weight of the graph, added for system stabilisation.

## IV. Experiment Results

In this section, we provide experimental examples to validate the advantage of proposed heart rate estimation algorithm.

### A. Experiment setup

The UWB impulse radar sensor is the Xethru X4M03 development kit. The detailed hardware design can be found in reference [16]. For performance demonstration, we consider the time-frequency (2-D) analysis since we are observing a time-varying process. Some of the key radar parameters are summarized in Table I.

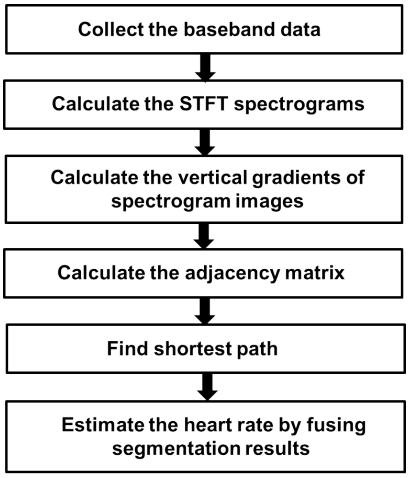


Fig. 1. The flowchart of the graph-based method for heart rate trace estimation

.

TABLE I
SYSTEM PARAMETERS

| Specification | Values |
|---|---|
| Center frequency | 7.29 GHz |
| Bandwidth | 1.4 GHz |
| Fast-time sampling rate after coherent combing | 20 HZ |
| Coherent processing time | 15 s |

### *B. Heart rate trace results*

The following results are generated from one 260-s data set with a 15-s processing window and 1-s increment each processing time. Gaussian filtering is performed to decrease the noise. To validate performance of estimation method, the corresponding PPG signal are also recorded and collected as reference. Fig. 2 shows the spectrograms visualization of PPG reference data, complex data and phase data, respectively. Both the fundamental heart rate and second order harmonic signal are clearly visible in PPG data as layered structure in Fig. 2(a). Due to respiration interference, the heart rate and second order harmonic signal in complex data as shown in Fig. 2(b) are much weaker than these in PPG data. There only exists fundamental heart signal in phase data as shown in Fig. 2(c). Fig. 3 illustrates the segmentation results of graph based method by both complex and phase data. The estimation results of fundamental heart rate and second order harmonic are marked in white dotted lines in Fig. 3(a). The estimation result of fundamental heart rate is marked in white dotted line in Fig. 3(b).

The estimation results by different methods are compared in Fig. 4 including conventional method, graph based method and PPG reference. Conventional method is peak finding result. We also compare the heart rate estimation results by graph-based method with and without harmonic signal. Without harmonic signal, we only use the fundamental signal. With harmonic signal, we fuse fundamental result and harmonic signal by evenly weighted. Fig. 4(a) and (b) show different methods comparison by complex data and phase data, respectively. In general, the graph-based method shows better agreement with reference result than the peak finding method. The result of conventional method fluctuates a lot, which is more easily effected by respiration inference. In addition, the complex data shows performance advantage over phase data. The numerical analyses are given in the next subsection.

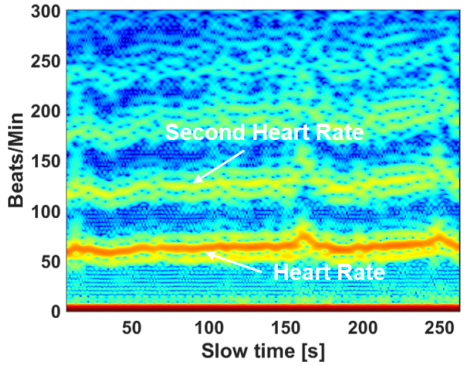


(a) PPG data

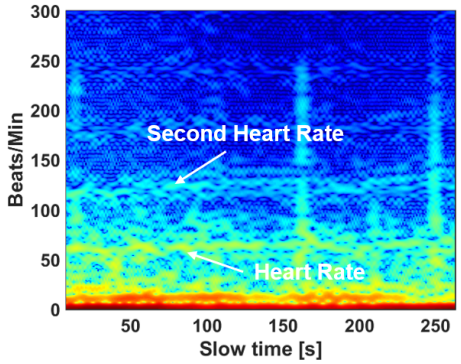


(b) Complex data

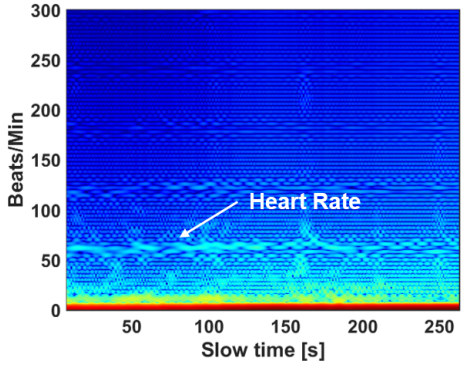


(c) Phase data

Fig. 2. Spectrograms visualization of complex and phase data: (a) is ppg reference data; (b) is the complex data; (c) is phase data.

### *C. Numerical analysis*

We utilized two evaluation metrics to characterize the algorithm performance, root mean square error ($RMSE$) and Pearson Correlation Coefficient ($PCC$). $RMSE$ is the squared and averaged difference between the estimated data and corresponding reference data. $PCC$ is to assess the similarity between the estimated data and corresponding reference

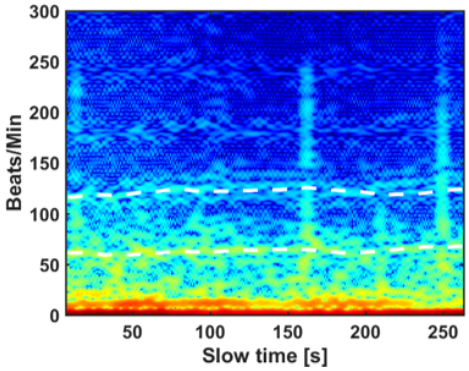


(a) Complex data

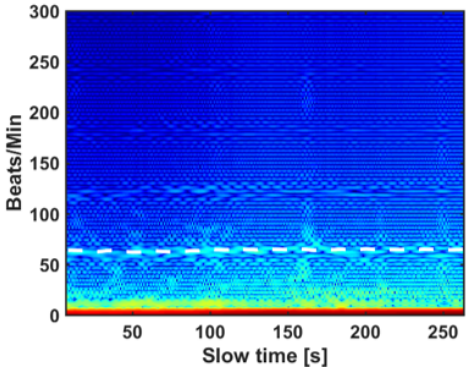


(b) Phase data

Fig. 3. Estimation results of graph based method by complex and phase data: (a) is the estimation result by complex data; (b) is the estimation result by phase data.

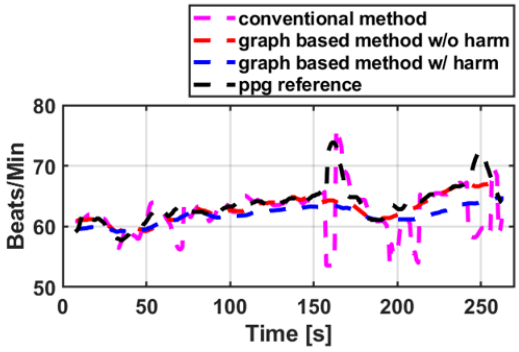


(a) Complex data

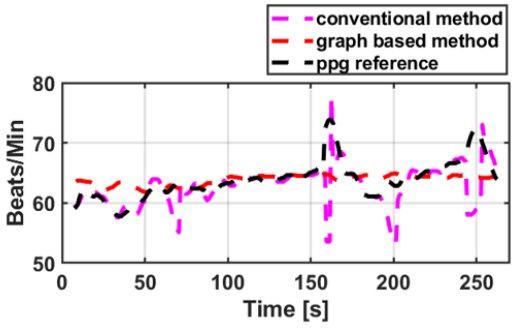


(b) Phase data

Fig. 4. Different results of heart rate trace estimation: (a) is the estimation result by complex data; (b) is the estimation result by phase data.

data. Table II gives the numerical performance comparisons between the graph-based method and conventional peak detection method. Both the complex data and phase data are evaluated. It is obvious the graph based method have higher $PCC$ and lower $RMSE$ than conventional method by no matter the complex data or phase data. It is worth noting that $PCC$ values are relatively small in conventional method, which means the poor estimation performance. Our method shows advantages of estimation than peak detection method. According to the performance comparison between complex and phase data in Table II, there are higher $PCC$ and lower $RMSE$ by complex data than by phase data.

To analysis the benefit of harmonic signal, Table III shows the comparison of estimation results with (w/) and without (w/o) the harmonic signal. The $PCC$ value with harmonic signal is bigger than without harmonic signal, which means better coherence over the whole data. The $RMSE$ value w/ harmonic signal is bigger than w/o harmonic signal. What's more, we also compare their performance including graph method w/o harmonic, graph method w/ harmonic and conventional method using every 10 seconds data . Both the $RMSE$ and $PCC$ are illustrated in Fig. 5(a) and Fig. 5(b), respectively. We can conclude that graph-based method performs well in the situation of obvious background inference and the harmonic signal is also helpful when the fundamental heart rate signal is masked or not available.

TABLE II
Comparisons between graph based method and conventional method

| Metric / Data | Graph method | | Conventional method | |
|---|---|---|---|---|
| | $PCC$ | $RMSE$ | $PCC$ | $RMSE$ |
| Complex Data | 0.7856 | 2.1202 | -0.2114 | 6.9915 |
| Phase Data | 0.4841 | 2.8215 | 0.3999 | 3.0157 |

TABLE III
Comparisons with and without harmonic signal

| Metric / Data | w/o harm | w/ harm |
|---|---|---|
| $PCC$ | 0.7856 | 0.8095 |
| $RMSE$ | 2.1202 | 2.9912 |

## V. Conclusion

Graph-based method outperforms the conventional estimation method in both the complex data and phase data. Compared with conventional method, the graph-based method is more robust to respiration interference. The complex data is more suitable to estimate the heart rate when paired with graph-based technique because of the harmonic information. The promising results show the potential of image-based method to improve UWB impulse radar heart rate estimation.

## References

[1] K. C. Peng, M. C. Sung, F. K. Wang and T. S. Horng, "Noncontact vital sign sensing under nonperiodic body movement using a novel frequency-locked-loop radar," IEEE Transactions on Microwave Theory and Techniques, vol. 69, no. 11, pp. 4762-4773, 2021.

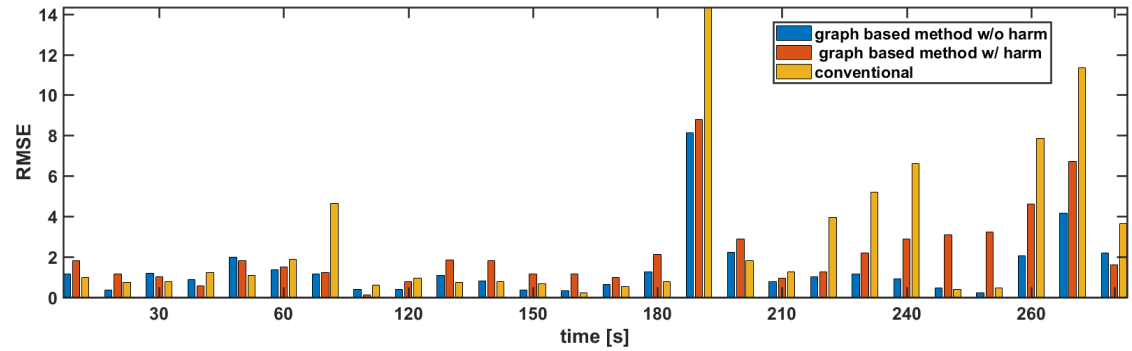


(a) $RMSE$ comparison

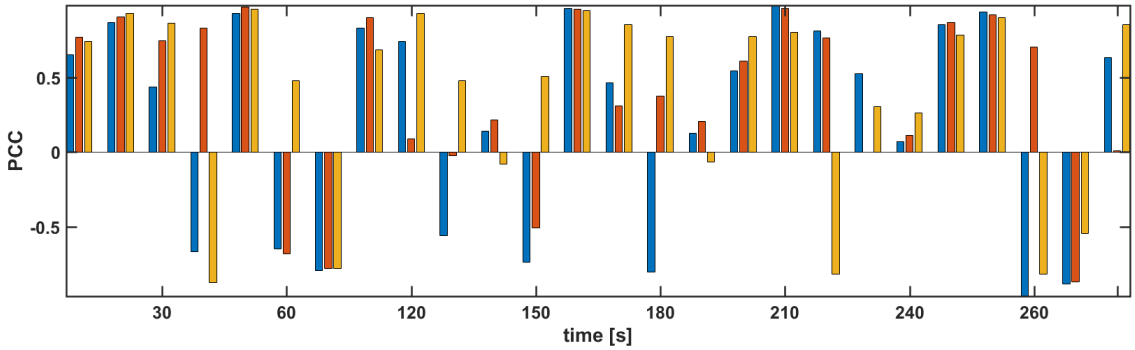


(b) $PCC$ comparison

Fig. 5. Performance comparisons of different estimation method by complex data: (a) is $RMSE$ comparison and (b) is $PCC$ comparison.


[2] A. T. Purnomo, K. S. Komariah, D. B. Lin, W. F. Hendria, B. K. Sin and N. Ahmadi, "Non-contact supervision of COVID-19 breathing behaviour with FMCW radar and stacked ensemble learning model in real-time," IEEE Transactions on Biomedical Circuits and Systems, vol. 16, no. 4, pp. 664-678, 2022.

[3] J. Li, Z. Zeng, J. Sun, and F. Liu, "Through-wall detection of human being's movement by UWB radar," IEEE Geoscience and Remote Sensing Letters, vol. 9, no. 6, pp. 1079–1083, 2012.

[4] Y. Wang, Q. Liu, and A. E. Fathy, "CW and pulse–Doppler radar processing based on FPGA for human sensing applications," IEEE Transactions on Geoscience and Remote Sensing, vol. 51, no. 5, pp. 3097–3107, 2013.

[5] Y. Rong and D. W. Bliss, "Harmonics-based multiple heartbeat detection at equal distance using UWB impulse radar," 2018 IEEE Radar Conference (RadarConf18), Oklahoma City, OK, USA, 2018, pp. 1101-1105.

[6] C. Li and J. Lin, "Complex signal demodulation and random body movement cancellation techniques for non-contact vital sign detection," Microwave Symposium Digest, 2008 IEEE MTT-S International, 2008, pp. 567–570.

[7] B. K. Park, O. Boric-Lubecke, and V. M. Lubecke, "Arctangent demodulation with DC offset compensation in quadrature doppler radar receiver systems," IEEE transactions on Microwave theory and techniques, vol. 55, no. 5, pp. 1073–1079, 2007.

[8] J. Wang, X. Wang, L. Chen, J. Huangfu, C. Li, and L. Ran, "Noncontact distance and amplitude-independent vibration measurement based on an extended DACM algorithm," IEEE Transactions on Instrumentation and Measurement, vol. 63, no. 1, pp. 145–153, 2014.

[9] Y. Rong and D. W. Bliss, "Remote sensing for vital information based on spectral-domain harmonic signatures," IEEE Transactions on Aerospace and Electronic Systems, vol. 55, no. 6, pp. 3454-3465, Dec. 2019, doi: 10.1109/TAES.2019.2917489.

[10] Y. Rong and D. W. Bliss, "Smart homes: See multiple heartbeats through wall using wireless signals," 2019 IEEE Radar Conference (RadarConf), Boston, MA, USA, 2019, pp. 1-6.

[11] S. J. Chiu, X. T. Li, P. Nicholas, C. A. Toth, J. A. Izatt, and S. Farsiu, "Automatic segmentation of seven retinal layers in SDOCT images congruent with expert manual segmentation," Optical Express, vol. 18, pp. 19413-19428, 2010.

[12] X. Yang, Z. Zhang, Y. Huang, Y. Zheng, Y. Shen, "Using a graph-based image segmentation algorithm for remote vital sign estimation and monitoring," Scientific Report, vol.12, no.1, pp.15197, 2022.

[13] Graph-based segmentation of retinal layers in OCT images (MATLAB MATLAB Central File Exchange, 2021).

[14] E. Sejdić, I. Djurović, and J. Jiang, "Time–frequency feature representation using energy concentration: An overview of recent advances," Digital Signal Processing, vol. 19, no. 1, pp. 153–183, 2007.

[15] E. Jacobsen and R. Lyons, "The sliding DFT," Signal Processing Magazine, vol. 20, no. 2, pp. 74–80, 2003.

[16] N. Andersen, K. Granhaug, J. A. Michaelsen, S. Bagga, H. A. Hjortland, M. R. Knutsen, T. S. Lande, and D. T. Wisland, "A 118-mW pulse-based radar SoC in 55-nm CMOS for non-contact human vital signs detection," IEEE Journal of Solid-State Circuits, vol. 52, no. 12, pp. 3421-3433, 2017.